

*Full Length Research Paper*

# Simulating of microstructure and magnetic properties of nanostructured Fe and Fe<sub>50</sub>Co<sub>50</sub> powders by neural networks

Ali Heidari<sup>1\*</sup>, Mehdi Delshad Chermahini<sup>2</sup> and Mohammad Heidari<sup>3</sup>

<sup>1</sup>Department of Civil Engineering, Shahrekord University, Shahrekord, Iran.

<sup>2</sup>Department of Material Science and Engineering, Kerman University, Kerman, Iran.

<sup>3</sup>Islamic Azad University, Aligodarz Branch, Aligodarz, Iran.

Accepted 27 August, 2010

In this study, a series of experiments were performed in order to determine the effects of changing milling time on the microstructure and magnetic properties of nanostructured Fe and Fe<sub>50</sub>Co<sub>50</sub> alloys by back propagation neural networks (BPN). The microstructure and magnetic properties of Fe and Fe<sub>50</sub>Co<sub>50</sub> alloys were estimated using the data acquired from the experiments performed, performance values obtained were used for training a BPN whose structure was designed for this operation. The network, which has two layers as hidden layer, and output layer, has two input and five output neurons. The BPN is used for simulating the microstructure and magnetic properties of nanostructured Fe and Fe<sub>50</sub>Co<sub>50</sub> alloys. The BPN method is found to be the most accurate and quick, the best results were obtained by the BPN by quasi-newton algorithms training with 12 neurons in the hidden layer. The quasi-newton algorithms procedure is more accurate and requires significantly less computation time than the other methods. Training was continued until the mean square error is less than 1e-3, desired error value was achieved in the BPN was tested with both data used and not used for training the network. Resultant of the test indicates the usability of the BPN in this area.

**Key words:** Nanostructured materials, mechanical alloying, microstructure, magnetic measurements, computer simulation.

## INTRODUCTION

It is established that during mechanical alloying a solid state reaction takes place between the fresh powder surfaces of the reactant materials at room temperature. Consequently, it can be useful to produce alloys and compounds that are difficult and impossible to be obtained by conventional melting and casting techniques (Capdevila et al., 2001).

Pure iron is a good ferromagnetic material with a low resistivity so in some applications it leads to large eddy current losses. Alloying can be engineered to instill greater magnetic permeability and lower core losses (Koohkan et al., 2008). Cobalt in iron is unique in increasing simultaneously the saturation magnetization and Curie temperature (McHenry et al., 1999). Although

the maximum saturation magnetization ( $M_S$ ) occurs at a concentration of 35 at % Co, equiatomic compositions offer a considerably larger permeability for similar  $M_S$  (Sourmail, 2005). Recently, the effects of milling time (Delshad Chermahini et al. 2009a), composition (Delshad Chermahini et al., 2009c), heating time (Delshad Chermahini and Shokrollahi, 2009) and heating rate (Delshad Chermahini et al., 2009b) on the both microstructure and magnetic properties of nanostructured Fe-Co alloys were investigated. The present paper is focused on the prediction effect of the ball milling on the structure and the magnetic properties of Fe and Fe<sub>50</sub>Co<sub>50</sub> alloys, using artificial neural network.

The structure and magnetic properties of Fe and Fe<sub>50</sub>Co<sub>50</sub> alloys in the experiments were adjusted by changing the milling time. Then the data obtained from the test results was used for simulating the system performance by the BPN. Recent developments in

\*Corresponding author. E-mail: [heidari@eng.sku.ac.ir](mailto:heidari@eng.sku.ac.ir).

**Table 1.** Experimental measurements.

Milling time	Fe					Fe <sub>50</sub> Co <sub>50</sub>				
	Cry	Mic	Lat	Coe	Mag	Cry	Mic	Lat	Coe	Mag
0.3	101	0.03	0.28669	25.0	208.1	100	0.04	0.28650	72.0	178.0
1.0	72	0.06	0.28673	27.0	208.3	68	0.08	0.28649	79.0	179.0
1.5	50	0.15	0.28677	29.0	208.5	40	0.20	0.28648	85.0	180.0
2.0	45	0.23	0.28680	30.0	208.7	35	0.33	0.28648	94.0	181.0
3.0	40	0.30	0.28686	34.0	209.0	30	0.45	0.28642	103.0	182.0
4.0	35	0.47	0.28692	33.0	209.1	25	0.63	0.28637	97.8	189.0
5.0	30	0.66	0.28698	32.0	209.2	21	0.86	0.28631	92.6	196.0
6.0	23	0.79	0.28703	31.3	209.3	17	1.00	0.28626	87.5	200.0
7.0	18	0.90	0.28707	30.6	209.4	15	1.10	0.28623	78.7	204.0
8.0	14	1.00	0.28710	30.0	209.5	12	1.20	0.28620	70.0	208.0
12.0	13	1.13	0.28719	29.3	209.7	11	1.23	0.28617	67.0	208.7
17.0	12	1.17	0.28727	28.6	209.9	12	1.23	0.28616	64.0	209.4
20.0	12	1.20	0.28730	28.0	210.0	12	1.20	0.28615	61.0	210.0
26.0	13	1.20	0.28732	27.4	210.3	12	1.18	0.28613	60.6	211.7
30.0	12	1.21	0.27834	26.7	210.6	12	1.16	0.28611	60.3	213.4
35.0	13	1.20	0.28735	26.0	211.0	12	1.15	0.28610	60.0	215.0
37.0	15	1.15	0.28736	25.1	211.2	12	1.11	0.28610	57.0	215.6
40.0	17	1.09	0.28736	24.2	211.4	13	1.06	0.28611	54.0	216.2
43.0	18	1.02	0.28737	23.1	211.7	14	1.00	0.28612	51.0	216.8
45.0	19	0.95	0.28737	22.0	212.0	15	0.95	0.28613	47.0	217.5

information technology and increased computer powers led to the development of new programming techniques.

One kind of artificial neural network is BPN. The BPN are being used in control applications, robots, pattern recognition, medicine, power systems, signal processing, social and psychological sciences. The BPN have also being used in heating (Rama Kumar and Prasad, 2006), cooling (Kanarachos and Geramanis, 1998), analysis (Swider et al., 2001), design (Heidari and Salajegheh, 2006; Heidari and Karimpor, 2008; Heidari et al., 2009) and optimization (Salajegheh and Heidari 2004a, b).

## EXPERIMENTAL DETAILS

Fe (99.5%, < 10 μm) and Co (99%, < 3 μm) powders supplied by Merck were mechanically alloyed in an argon atmosphere to form Fe and Fe<sub>50</sub>Co<sub>50</sub> alloy in a Fritsch planetary ball mill, whilst confined in sealed 250 ml steel containers rotated at 400 rpm for a variety of milling times. The container was loaded with a blend of balls (φ = 10 mm, mass = 4.14 g and φ = 20 mm, mass = 32.12 g). The total weight of the powder was about 23 g and the ball to powder mass ratio was about 20:1.

X-ray diffraction measurements were carried out in a Philips X'Pert High Score diffractometer using Cu K<sub>α</sub> (λ = 1.5405 Å) radiation over 2θ = 20 - 140°. The crystallite size and lattice strain were estimated using the Williamson-Hall method:

$$B_s \cos \theta = 2(\mathcal{E}) \sin \theta + k/\lambda D$$

Where  $B_s$  is the full-width at half maximum of the diffraction peak,  $\theta$  is the Bragg angle,  $\mathcal{E}$  is the internal microstrain  $\lambda$  is the wavelength of the X-ray,  $D$  is the crystallite size.  $B_s$  can be given as

$$B_s^2 = B_m^2 - B_c^2$$

Where  $B_s$  is the width at half-maximum of the Si powder peaks used for calibration and  $B_m$  is the evaluated width.

Lattice parameters were determined using 3 high-angle peaks in order to increase the precision of the measurements. Morphology and particle size were observed using scanning electron microscopy (Camscan mv2300). Magnetic properties were estimated using a magnetometer VSM.

The used data for this paper is prepared by the author at previous work (Delshad Chermahini et al., 2009a). The effect of milling time on the microstructure (crystallite size, microstrain and lattice parameter) and magnetic properties (coercivity and magnetization saturation) of nanostructured Fe and Fe<sub>50</sub>Co<sub>50</sub> powders has been investigated. The results of this experimental study are shown in Table 1, where Cry is crystallite size, Mic is microstrain, Lat is lattice parameter, Coe is coercivity and Mag is magnetization saturation.

For each composition (Fe and Fe<sub>50</sub>Co<sub>50</sub>), 20 milling times are selected. The experimental results that are shown in Table 1 were conducted on the system by changing the milling time is used to train and test of the BPN (Delshad Chermahini et al., 2009a).

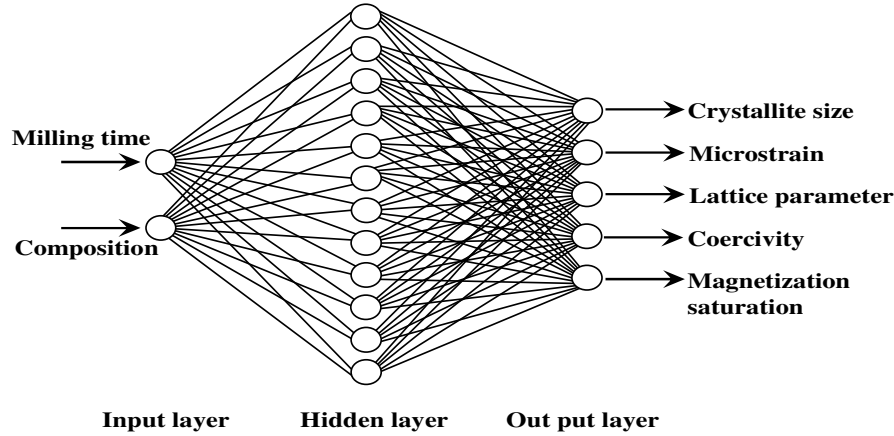


Figure 1. Architecture of the BPN used.

**BACK PROPAGATION NEURAL NETWORK**

Back propagation neural network resembling neural neurons of a human brain are used successfully in many science branches on modelling and control applications. The BPN can be used to learn from the training dataset the non-linear relationships between multiple inputs and outputs without requiring specific information on the fundamental mechanisms relating them. The BPN is composed of interconnected computational processing elements called neurons that process input information and give outputs. The BPN have an algorithm that can learn and decide by its own throughout the process. They have data processing units called neurons. These networks involve connections between the neurons, which have their own weights. Their total energy is calculated by multiplying data signals by these weights. Data at the neuron output is found by making use of an activation function. The BPN have structural and mathematical variations (Heidari and Karimpour, 2008; Salajegheh and Heidari, 2004a; Salajegheh and Heidari, 2004b).

Structural differences arise from the number of layers and the variations of the connections among the nodes. Generally, they have two layers as; hidden layer and output layer. Number of the layers can change and can be rebounded between the layers. This completely depends on the usage purpose of the network. Number of the nodes in the input equals to the number of data to be given to the BPN. Number of nodes at the output layer equals to the number of knowledge that will be taken from the BPN (Figure 1).

Learning capability of the BPN improves as the number of nodes and the connections increases; however, it takes more time to train. A node has many inputs while it has only one output. Nodes process these input data and feed forward to the next layer. Input data are processed as follows; each data are added up after it was multiplied by its weight and then it is subjected to activation function. Thus, the data, which will be transferred to the next layer, is obtained. The algorithm used in training the BPN, and the type of activation function used at the output of the node are the mathematical differences. Activation functions involve exponential functions and thus non-linear modeling can be achieved. Various algorithms have been developed according to the BPN purpose of usage. They can be preferred according to their convenience to the problem to be solved, and training speed. The BPN are trained with known data and then tested with data not used in training. Although training takes a long time, they make decisions very fast during operation. They are used widely in simulating non-linear systems thanks to their ability to learn, generalize, tolerate the faults and benefit from the faulty samples. In the BPN optimizes the weighted connections by allowing the error to spread from output layer

towards the lower layers, was used as the training system in training networks. The values of the training and test data were normalized to a range from -1 to 1. The formulas used in this algorithm are as follows (Heidari, 2008):

i.) Hidden layer calculation results:

$$net_i = \sum x_i w_i \tag{1}$$

$$y_i = f(net_i) \tag{2}$$

Where  $x_i$  and  $w_i$  are input data and weights of the input data, respectively.  $f$  is activation function, and  $y_i$  is result obtained from hidden layer.

ii.) Output layer calculation results:

$$net_k = \sum y_i w_{jk} \tag{3}$$

$$o_k = f(net_k) \tag{4}$$

Where  $w_{jk}$  are weights of output layer and  $o_k$  is result obtained from output layer.

iii.) Activation functions used in layers are tansig and linear (Heidari, 2008):

$$f(net_i) = \frac{1 - e^{-net_i}}{1 + e^{-net_i}} \text{ (tansig)} \tag{5}$$

$$f(net_i) = net_i \text{ (linear)} \tag{6}$$

iv.) Errors made at the end of one cycle:

$$e_k = (t_k - o_k) o_k (1 - o_k) \tag{7}$$

$$e_i = y_i (1 - y_i) \sum e_k w_{ij} \tag{8}$$

**Table 2.** Result of neural network with the BPN for Fe.

Milling time	Fe (Neural network)					Error = (Exp - Neu)/Exp × 100				
	Cry	Mic	Lat	Coe	Mag	Cry	Mic	Lat	Coe	Mag
1.0	74.2	0.062	0.28645	26.89	209.29	3.06	3.33	0.097	0.41	0.44
6.0	22.13	0.76	0.28702	31.82	210.61	3.78	3.79	0.004	1.66	0.63
17.0	12.34	1.16	0.28728	28.12	209.46	2.83	0.85	0.004	1.68	0.21
30.0	12.13	1.24	0.28743	25.93	211.61	1.08	2.47	0.035	4.53	0.48
40.0	16.63	1.12	0.28738	24.43	212.32	2.18	2.75	0.007	0.95	0.44
Mean relative error for the data not used in training						2.59	2.64	0.029	1.52	0.45

Where  $t_k$  is result expected from output layer,  $e_k$  is error occurred at output layer, and  $e_i$  is error occurred at hidden layer.

v.) Weights can be changed using these calculated error values according to:

$$w_{jk} = w_{jk} + \alpha e_k y_i + \beta \Delta w_{jk} \quad (9)$$

$$w_{ij} = w_{ij} + \alpha e_i x_i + \beta \Delta w_{ij} \quad (10)$$

Where  $w_{jk}$  and  $w_{ij}$  are weights of output and hidden layers, respectively.  $\Delta w_{jk}$  and  $\Delta w_{ij}$  are correction made in weights at the previous calculation.  $\alpha$  is learning ratio and  $\beta$  is momentum, that is used to adjust weights. In this paper,  $\alpha = 0.75$  and  $\beta = 0.70$ , are used.

vi.) Square error, occurred in one cycle, can be found by Eq. 11.

$$e = \sum 0.5 |t_k - o_k|^2 \quad (11)$$

vii.) The completion of training the BPN, relative error (RE) for each data and mean relative error (MRE) for all data are calculated according to Eqs. 12 and 13, respectively.

$$RE = \left( \frac{100 (t_k - o_k)}{t_k} \right) \quad (12)$$

$$MRE = \frac{1}{n} \sum_{i=1}^n \left( \frac{100 (t_k - o_k)}{t_k} \right) \quad (13)$$

Where  $n$  is the number of data.

## RESULTS AND DISCUSSION

Thirty out of forty experiments results used in training and the other 10 experiments were used to test of the BPN. Square error condition of less than  $1e-3$  was tried to be realized in training and it was achieved for the BPN. The various training algorithm (Heidari, 2008) is used for training the BPN. All weights were corrected and

repeated after the calculation of each data set. The best algorithm for this problem is the quasi-Newton algorithms. This is the type of problem for which the quasi-newton algorithms is best suited. A personal computer Pentium 4 is used and the computing time is calculated in clock time. The BPN with twelve hidden neuron reached to desired error value after repeating 4.23 s.

No more the BPN having hidden layer neurons other than this number was tested since the desired error value was reached by this the BPN. Relative error values were calculated for the data used and not used in training according to Equations 12 and 13. Crystallite size, micro-strain, lattice parameter, coercivity and magnetization saturation error values of these (RE, MRE) found by artificial neural network with the BPN as well as. The test and RE values can be seen in Tables 2 and 3. Crystallite size, micro-strain, lattice parameter, coercivity and magnetization saturation predicted by the BPN and the experimental results were compared in Figures 2 - 6. Apses of the graphic shows the values measured, and estimated by the BPN. The regression value ( $R^2$ ) of the output variable values between the experimental values and the values estimated by the BPN were also calculated.

Figure 2 shows the changes in crystallite size. The BPN learned the data not used in training with a MRE of 2.19% and a regression value of 0.9881. The change in microstrain is shown in Figure 3. Mean relative error of the BPN in these values is 2.42% and regression value is 0.9804. The lattice parameter is shown in Figure 4. The BPN learned the data not used in training with a MRE of 0.025% and a regression value of 0.9992. The coercivity is shown in Figure 5. The BPN learned the data not used in training with a MRE of 1.41% and a regression value of 0.9955. The magnetization saturation is shown in Figure 6. The BPN learned the data not used in training with a MRE of 0.31% and a regression value of 0.9979.

## CONCLUSION

Microstructural and magnetic properties estimation was made according to the experimental values by using the BPN. Results of 30 experiments out of 40, which were conducted at laboratory conditions, were used to train the

**Table 3.** Result of neural network with the BPN for Fe<sub>50</sub>Co<sub>50</sub>.

Milling time	Fe <sub>50</sub> Co <sub>50</sub> (Neural network)					Error = (Exp - Neu)/Exp × 100				
	Cry	Mic	Lat	Coe	Mag	Cry	Mic	Lat	Coe	Mag
2.0	36.21	0.34	0.28645	93.23	181.44	3.46	3.03	0.011	0.82	0.24
5.0	20.62	0.84	0.28613	91.81	195.91	1.81	2.32	0.063	0.85	0.05
20.0	12.11	1.19	0.28611	62.15	210.83	0.92	0.83	0.014	1.89	0.39
37.0	12.17	1.09	0.28612	56.91	215.29	1.42	1.80	0.007	0.16	0.14
43.0	13.81	0.97	0.28614	52.43	216.7	1.36	3.00	0.007	2.80	0.05
Mean relative error for the data not used in training						1.79	2.20	0.020	1.30	0.17

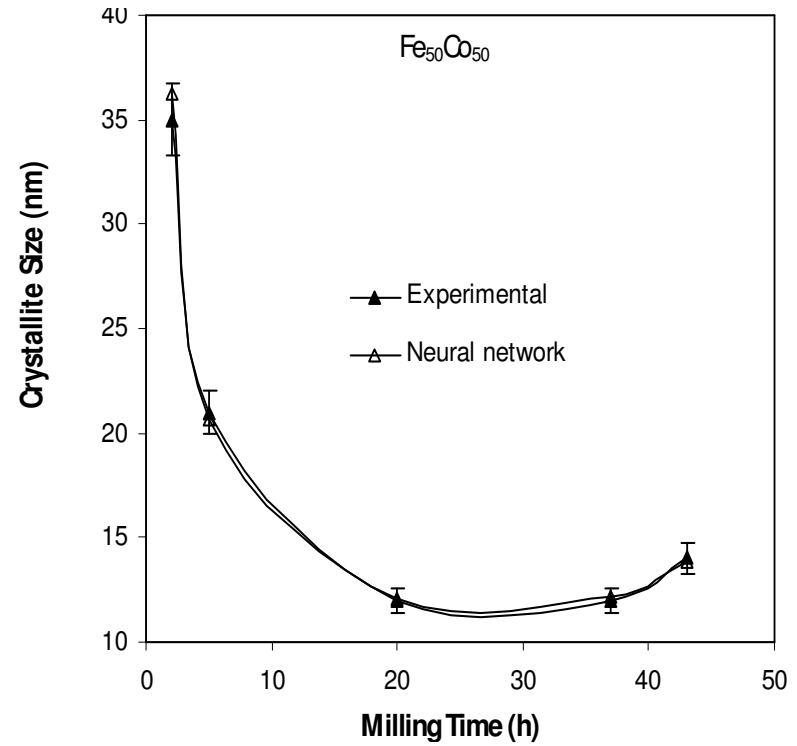
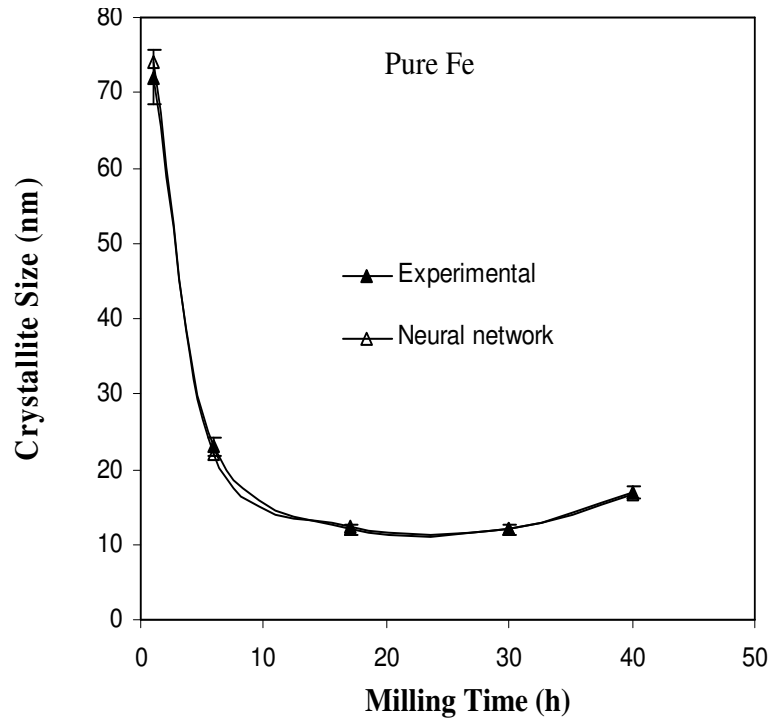


**Figure 2.** (a) The crystallite size of pure Fe from the experimental data, and the one obtained from neural network. (b) The crystallite size of Fe<sub>50</sub>Co<sub>50</sub> from the experimental data, and the one obtained from neural network.

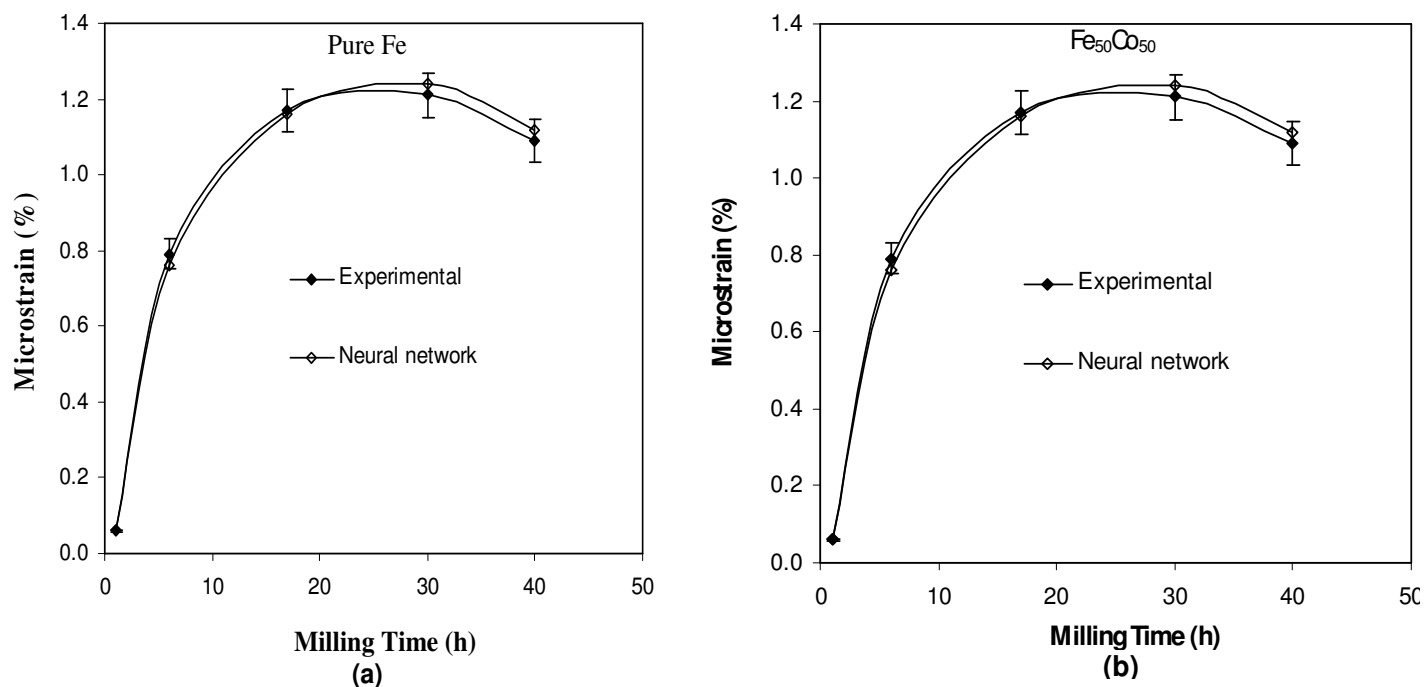


**Figure 3.** (a) The microstrain of pure Fe from the experimental data, and the one obtained from neural network. (b) The microstrain of Fe<sub>50</sub>Co<sub>50</sub> from the experimental data, and the one obtained from neural network.

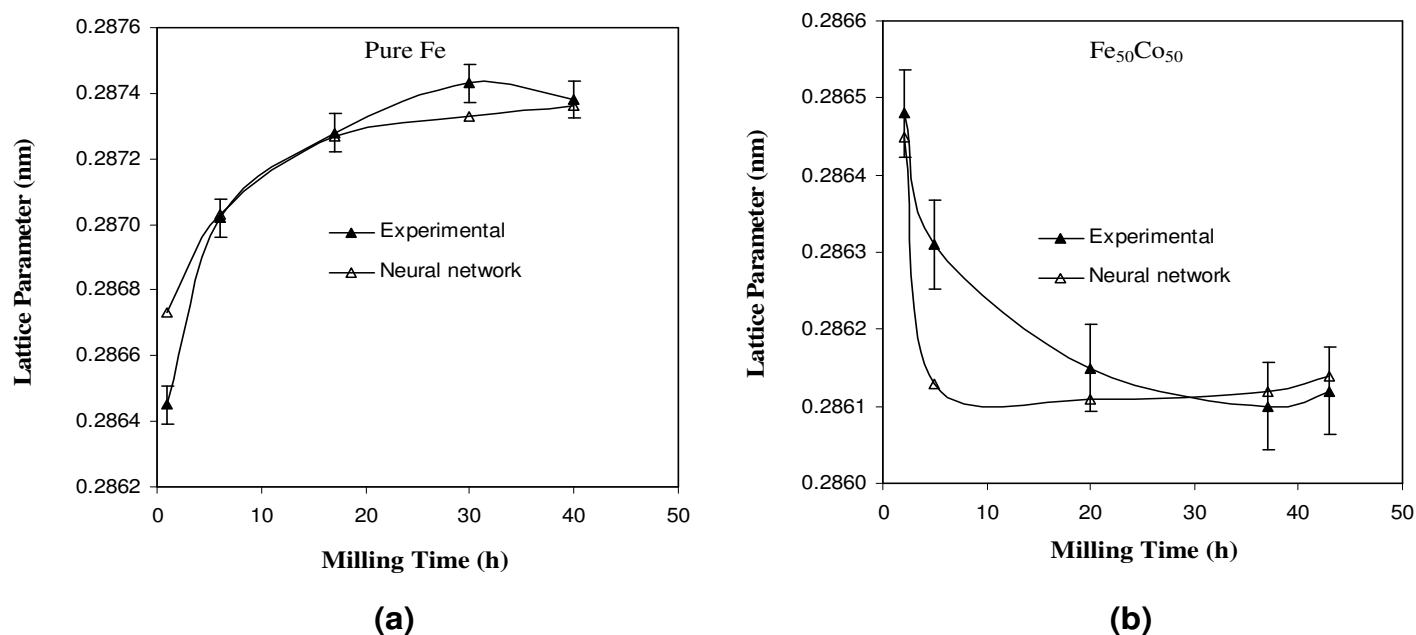


**Figure 4.** (a) The lattice parameter of pure Fe from the experimental data, and the one obtained from neural network. (b) The lattice parameter of Fe<sub>50</sub>Co<sub>50</sub> from the experimental data, and the one obtained from neural network.

BPN and the other 10 were used to test the BPN. Mean relative errors of the test of artificial neural network were found to be 2.19% for crystallite size, 2.42% for microstrain, 0.025% for lattice parameter, 1.41% for

coercivity and 0.31% for magnetization saturation. Multiple determination coefficient found by the BPN were 0.9881 for crystallite size, 0.9804 for microstrain, 0.9992 for lattice parameter, 0.9955 for coercivity and 0.9979 for

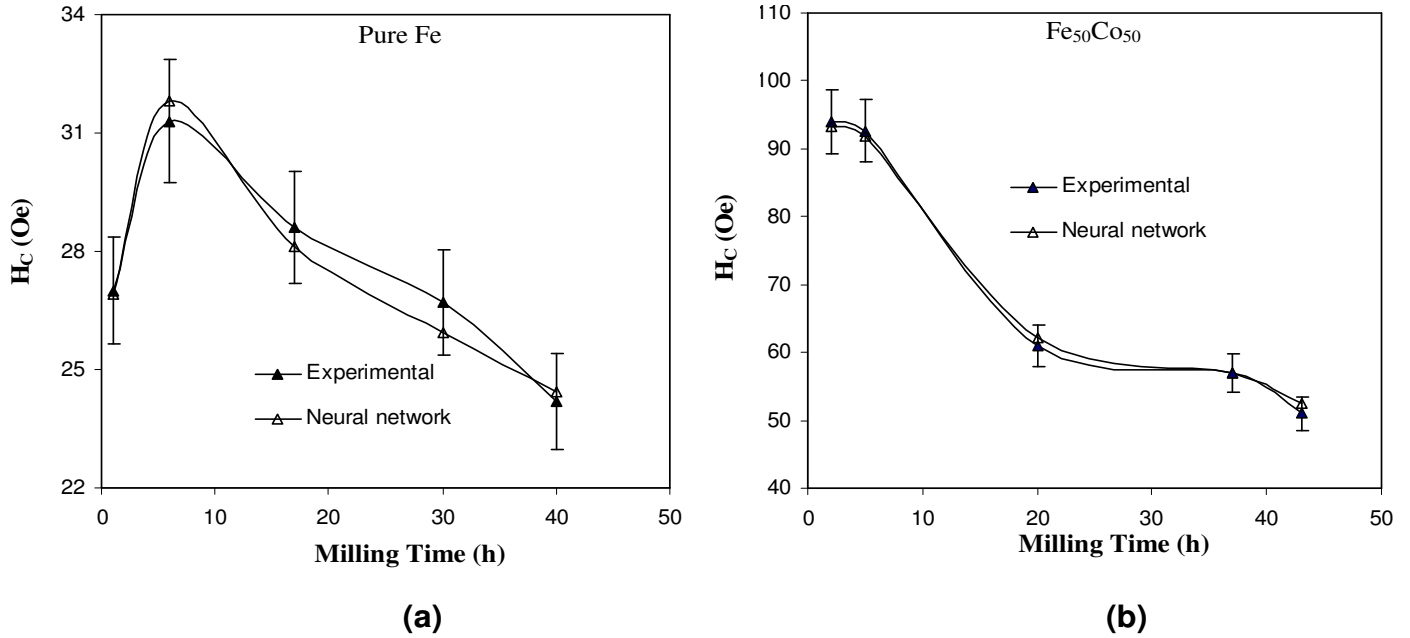


**Figure 5.** (a) The coercivity of pure Fe from the experimental data, and the one obtained from neural network. (b) The coercivity of Fe<sub>50</sub>Co<sub>50</sub> from the experimental data, and the one obtained from neural network.

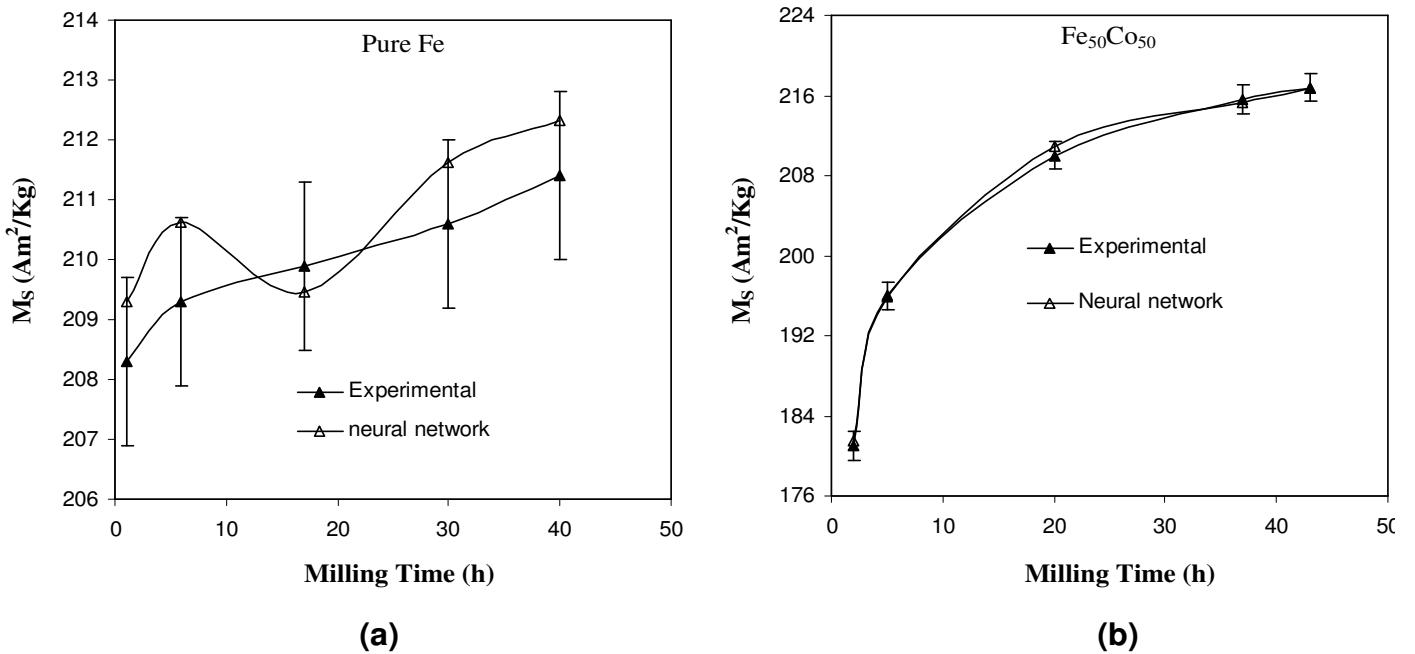


**Figure 6.** (a) The magnetization saturation of pure Fe from the experimental data, and the one obtained from neural network, (b) The magnetization saturation of Fe<sub>50</sub>Co<sub>50</sub> from the experimental data, and the one obtained from neural network.

magnetization saturation. These results showed that the BPN gave a good estimation of results and it can be used in performance estimation of microstructural and magnetic properties with appropriate network architecture and training set.

**REFERENCES**

Capdevila C, Miller U, Jelenak H, Bhadeshia HKDH (2001). Strain heterogeneity and the production of coarse grains in mechanically alloyed iron-based PM2000 alloy, Mater. Sci. Eng. A., 316: 161–165.  
 Delshad Chermahini M, Sharafi S, Shokrollahi H, Zandrahimi M

- (2009a). Microstructural and magnetic properties of nanostructured Fe and Fe<sub>50</sub>Co<sub>50</sub> powders prepared by mechanical alloying, *J. Alloys Comp.*, 474: 18-22.
- Delshad Chermahini M, Sharafi S, Shokrollahi H, Zandrahimi M, Shafiei A (2009b). The evolution of heating rate on the microstructural and magnetic properties of milled nanostructured Fe<sub>1-x</sub>Co<sub>x</sub> (x = 0.2, 0.3, 0.4, 0.5 and 0.7) powders, *J. Alloys Comp.*, (in press).
- Delshad Chermahini M, Zandrahimi M, Shokrollahi H, Sharafi S (2009c). The effect of milling time and composition on microstructural and magnetic properties of nanostructured Fe–Co alloys *J. Alloys Comp.*, 477: 45-50.
- Delshad Chermahini M, Shokrollahi H (2009). Milling and subsequent thermal annealing effects on the microstructural and magnetic properties of nanostructured Fe<sub>90</sub>Co<sub>10</sub> and Fe<sub>65</sub>Co<sub>35</sub> powders, *J. Alloys Comp.*, 480: 161-166.
- Heidari A (2008). Artificial neural network (theory and application with MATLAB), Nazeran, Esfahan, (in Farsi).
- Heidari A, Heidari M, Rahmani S (2009). Modelling Absorption Heat Transformer Powered by Back Propagation Neural Network, *J. Eng. Tech. Res.* (Submitted).
- Heidari A, Karimpor M (2008). Earth pressures and design of narrow MSE walls by neural network, 3<sup>rd</sup> International Conference on Bridge, Tehran, Iran.
- Heidari A, Salajegheh E (2006). Time history analysis of structures for earthquake loading by wavelet networks, *Asian J. Civil Eng.*, 7: 155-168.
- Kanarachos A, Geramanis K (1998). Multivariable control of single zone hydronic heating system with neural networks, *Energy Convers. Manage.*, 39: 1317-1328.
- Koohkan R, Sharafi S, Shokrollahi H, Janghorban K (2008). Preparation of nanocrystalline Fe–Ni powders by mechanical alloying used in soft magnetic composite, *J. Manage. Magn. Mater.*, 320: 1089-1094.
- McHenry ME, Willard MA, Laughlin DE (1999). Amorphous and nanocrystalline materials for applications as soft magnets, *Prog. Mat. Sci.*, 44: 291-433.
- Rama Kumar BVN, Prasad BVSSS (2006). A combined CFD and network approach for a simulated turbine blade cooling system, *Indian J. Eng. Mater. Sci.*, 13: 20-31.
- Salajegheh M, Heidari A (2004a). Optimum design of structures against earthquake by discrete wavelet neural network, 7<sup>th</sup> International Conference on Computational Structures Technology, Lisbon, Portugal.
- Salajegheh E, Heidari A (2004b). Optimum design of structures against earthquake by adaptive genetic algorithm using wavelet networks, *Struc. Multi. Optim.*, 28: 277-285.
- Sourmail T (2005). Near equiatomic FeCo alloys: Constitution, mechanical and magnetic properties, *Prog. Mater. Sci.*, 50: 816-880.
- Swider DJ, Browne MW, Bansal PK, Kecman V (2001). Modeling of vapour-compression liquid chillers with neural networks, *Appl. Therm. Eng.*, 21: 311-323.